A Two-Stage Fault Location Identification Method in Multiarea Power Grids Using Heterogeneous Types of Data

Iman Kiaei, *Member, IEEE*, and Saeed Lotfifard, *Senior Member, IEEE*

***Abstract*—This paper proposes a two-stage fault location method for multiarea power systems. It utilizes available heterogeneous types of data consisting of status data (i.e., discrete data) and analog data (i.e., continues data). A distributed casual model-based diagnosis method using P-invariant Petri nets is proposed that utilizes status data to find faulted sections. Each subsystem/area of multiarea power systems has its own diagnostic model and determines the diagnosis solution based on its local net, the local manifestations, and limited information exchange with the neighboring subsystems/areas. Once a short list of possible fault sections is determined, the second stage further improves the estimated fault location using analog data. The actual fault location is estimated by comparing the measured analog data with their associated calculated values in computer programs using short-circuit analysis algorithms. Simulation results demonstrate that the proposed distributed fault location method can diagnose faults in multiarea power systems accurately.**

***Index Terms*—Alarm processing, distributed model-based fault diagnosis, fault location, Petri nets, synchronized phasor measurement.**

I. Introduction

POWER grids as one of the most complex man-made systems are prone to various contingencies and faults. Protection systems that consist of protective relays, circuit breakers, and communication systems detect faults and isolate faulted components quickly to maintain the required reliability and security of power supply. During a major disturbance, system operators may face large number of alarms in few seconds [1]. For instance, thousands of sequences of event alarms were triggered at control centers in first 5 s after various faults in Hydro Quebec [2]. During postfault condition, the location of the fault should be determined quickly and accurately so that corrective actions are executed and further propagation of the event is prevented. Moreover, the information about the location of faults is required for the restoration of power systems [3].

Automated fault location methods assist power system operators in the decision-making process by providing synthetized and actionable information out of overwhelming amounts of collected raw data and measurements. The collected data from the supervisory control and data acquisition (SCADA) systems may include the status of protective relays and circuit breakers and analog data such as voltage and current signals. The measured data by phasor measurement units (PMUs) and conventional voltage and current meters can be used as well [4], [5]. To assure the fault location methods can be applied to a variety of protection schemes (digital, electronic, and electromechanical relays) and substations, different methods based on SCADA data have been proposed. Various fault location methods have been proposed that utilize status data for finding the faulted sections including model-based diagnosis (MBD) [6], rule-based diagnosis [7], expert systems [8], [9], analytical model [10], artificial neural networks [11], [12], Bayesian networks [13], data mining [14], rough sets [15], and cause–effect networks [16]. Logic-based expert systems have been proposed for fault diagnosis in [17] and [18]. The logic gates and Boolean functions are utilized to define the cause–effect model which suffers from heavy computation burden. The rule-based method requires large number of rules and training data to describe the behavior of power systems. On the contrary, in MBD methods, the decision of protective devices and fault clearance process is represented as discrete events to examine different fault scenarios [19]. To increase the speed of fault-diagnosis procedure, parallel processing techniques can be utilized [20]. Specifically, the Petri net method that is able to process the information in parallel and concurrent manners has been employed to increase the speed of diagnosis engine [21], [22]. Petri net fault-diagnosis models the power grid behavior precisely with clear physical interpretation and systematic reasoning procedure [23]–[25].

Analog data have also been used for fault location purpose in the past. For instance, in [26], voltage sag data generated by faults are used for the fault location purpose. In [27] and [28], faults location methods based on sparse measurement of voltage and/or current signals are proposed. In [29], a fault contour

Manuscript received September 7, 2018; revised October 26, 2018 and November 12, 2018; accepted November 30, 2018. Date of publication December 6, 2018; date of current version July 3, 2019. This work was supported in part by the U.S. National Natural Science Foundation under Grant 1840192. Paper no. TII-18-2334. *(Corresponding author: Saeed Lotfifard.)*

The authors are with the School of Electrical Engineering and Computer Science, Washington State University, Pullman, WA 99164 USA (e-mail: iman.kiaei@wsu.edu; s.lotfifard@wsu.edu).

Color versions of one or more of the figures in this paper are available online at http://ieeexplore.ieee.org.

Digital Object Identifier 10.1109/TII.2018.2885320

map is generated by utilizing the voltage and frequency signals for detecting and identifying the possible fault location. A comprehensive short-circuit analysis is performed by applying fault at every node of the grid and the prefault and postfault measurements are compared with the simulation results. The huge computation burden is the main shortcoming of the voltage sag algorithms [30], [31].

The aforementioned fault location methods have centralized architecture in which the casual model for the entire system is accessible and all of the final states are observable. In large-scale multiarea power grids that are spread over large geographical distance and are operated by different system operators, a centralized diagnosis system is not a suitable solution. To protect the confidentiality of the data, different power system operators prefer not to share all the data of their corresponding systems and prefer to minimize the required information exchange with the neighboring areas [32].

In power systems, different types of data coexist including status data, such as status of circuit breakers and output of protective relays, and analog data such as voltage and current signals measured by PMUs or conventional meters. Therefore, an optimal fault location should be proposed that takes full advantage of both types of data.

In this paper, a two-stage fault location method for multiarea power systems is proposed that utilizes both status and analog data for the fault location purpose and is implemented in a distributed architecture which makes it suitable for multiarea power systems. In the proposed method, a distributed MBD method based on P-invariant Petri net is proposed that utilizes status data to find the potential faulted sections. The Petri net diagnosis model of each area describes the behavior of local power system, protective relays, and operation status of circuit breakers. Upon occurrence of faults, the fault-diagnosis model of each area calculates a set of diagnoses based on the local manifestations and P-invariant offline net model. The local diagnoses contain the initial states that represent the cause of the observed symptoms. Since the local fault diagnosis is required to be consistent with the global reasoning, the result is checked among adjacent subsystems/areas and the inconsistent diagnoses are discarded from the diagnosis. Once a short list of faulted sections is generated by the first stage of the proposed fault location method, the estimated location of the fault is further narrowed down in the second stage. The analog data that include voltage and current signals measured by PMUs and conventional voltage and current meters installed throughout the power systems are utilized in the second stage. The fault location is estimated by comparing the measured analog data with the corresponding calculated values using short-circuit analysis algorithms.

This paper is organized as follows: Section II briefly explains the power system fault-diagnosis problem (DP) and provides a review of Petri net theory; Section III represents the process of distributed diagnosis; Section IV explains the details of the proposed fault location method; simulation results are provided in Section V; contributions of the developed technique are presented in Section VI; and conclusions are drawn in Section VII.

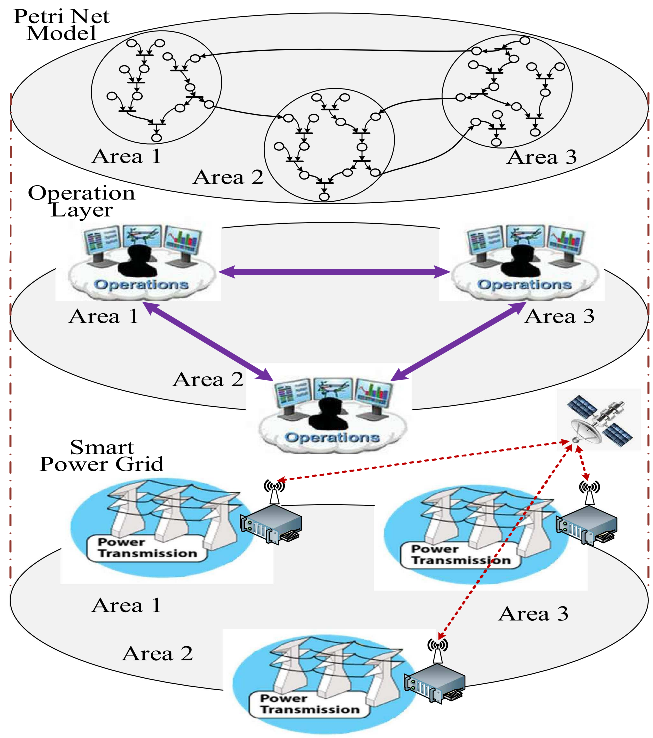

Fig. 1. Schematic diagram of the distributed fault-diagnosis process for multiarea power grid.

II. Fault DP

When a fault occurs in power systems, protection systems and circuit breakers operate to isolate the faulty component from the rest of the grid. Accurate and fast fault detection and fault location identification can accelerate the repair process of the system, provide the required information for emergency control of postcontingency systems, and expedite the restorative actions which decreases the outage time and increases the reliability of the system [33]. Performing fault reasoning in a short period of time for large interconnected power grids is a stressful and time-consuming task especially when multiple fault scenarios and failures of protective devices are involved. Practically, in multiarea power grids, the system operators of each area only have access to corresponding local observed signals and limited information exchange with the neighboring subsystems/areas. To address the above changes, in this paper, a distributed model-based fault diagnosis for multiarea power grid is developed. Fig. 1 shows the schematic diagram of the proposed method in which the fault-diagnosis processor at each subsystem performs the fault-diagnosis task based on the local model of the corresponding subsystem and limited information exchange with the neighboring subsystems to reach to the final results. The definition of fault diagnosis and configuration of the power system protection are explained in this part.

A. Fault-Diagnosis Algorithm

One of the main elements of a diagnosis process is causality analysis. The cause–effect relation among the system components is described by the directed graph. The casual model includes a set of nodes which are connected through the arcs [34]. The nodes are defined as follows.

1) *Initial nodes:* they are nodes that do not have any causes which means that no other nodes lead to these nodes. They are represented as source places and represent fault cases that lead to observations.
2) *Internal nodes:* correspond to the outcomes of the initial states. They have at least one parent and one child node in the graph.
3) *Manifestations:* they are observable symptoms of the system's malfunctions or failures. They are the last states in the model and indicate the sink nodes in the causal model.

The DP explains a manifestation by means of the initial states and is presented as follows [35]:

$$\mathrm{DP} = \left(\mathrm{NM}, \mathrm{Hyp}, \mathrm{Man}^{+}, \mathrm{Man}^{-}\right) \tag{1}$$

where NM represents the net model of the system under study, Hyp is a set of possible fault hypotheses whose elements are the possible cases of the observations, and Man^{+}, Man^{-} represents the manifestations. Man^{+} is a set of observations to be predicted by the diagnosis solution and Man^{-} denotes a set of undesired observations which are known to be absent in the examined case [7]. The diagnosis solution Δ (assumed as $\Delta \subseteq$ Hyp) is a set of the source nodes that are consistent with the manifestations that cover the elements of Man^{+} and zero-covers elements of Man^{-}. The logical representation of the diagnosis Δ for a specific reasoning problem can be expressed as follows:

$$\begin{aligned} &\forall\ w \in \mathrm{Man}^{+} : \mathrm{NM} \cup \Delta \vdash w \\ &\forall\ v \in \mathrm{Man}^{-} : \mathrm{NM} \cup \Delta \dashv v \end{aligned} \tag{2}$$

where $\vdash$ and $\dashv$ denote the derivation and not-derivation symbols, and *w* and *v* represent the elements of Man^{+} and Man^{-}, respectively.

B. Petri Net Model

Petri nets provide a systematic approach for modeling casuality in various processes. They describe the concurrency and parallelism aspects of information procedure through asynchronous systems such as protection systems of power grids. In this section, Petri net model is summarized. More details can be found in [36]–[40].

A Petri net is a triple structure $N = (P, T, F)$ with the following characteristics:

(i) $P = \{p_1, p_2, \ldots, p_m\}$ is a finite set of places.
(ii) $T = \{t_1, t_2, \ldots, t_m\}$ is a finite set of transitions.
(iii) $F \subseteq (P \times T) \cup (T \times P)$ is a set of arcs flow relations).
(iv) $P \cap T = \varphi$.
(v) $P \cup T = \{x \in P \cup T / \exists y : (xFy) \vee (yFx)\} \neq \varphi$.
(vi) $\mathrm{dom}\ (F)\ \cup \mathrm{cod}(F) = P \cup T$.
(vii) $x \in P \cup T, \quad {}^{\bullet}x = \{y | yFx\} \quad \text{and} \quad x^{\bullet} = \{y | xFy\}$ (3)

where ${}^{\bullet}x$ and $x^{\bullet}$ denote the input and output elements of places or transitions, respectively. The places and transitions are illustrated as circles and bars in the bipartite and directed graph. The transition set includes two subsets T_N and T_{OR}. The T_N (AND transitions) operates as a regular AND logic operator while the T_{OR} (OR transitions) represents the logical connective OR. A transition $t \in T_{\mathrm{OR}}$ is enabled if and only if at least one of its input places has one token. If the input subset of a place is empty ($|{}^{\bullet}x| = 0$), *x* is called source place and if its output subset is empty ($|x^{\bullet}| = 0$) *x* is called sink place. The initial marking of a Petri net is defined in M_0 set. A place is an element of a marking set, if it has a token. The dynamic characteristic of a net is defined by transferring tokens between places based on the enabling and firing rules of the transitions. (N, M_0) where *N* is Petri net and M_0 is a marked net. A transition $t \in T$ has concession in *M* (written as *M[t>*) if and only if all its input places have at least one token ($\forall p \in {}^{\bullet}t : M(p) \geq 1$). The marking M' is reachable if and only if it can be reached from a firing sequence τ such that $M[\tau > M'$. A marking *M* is called safe if $\forall p \in P,\ M(p) \leq 1$. The mapping between *n* transitions and *m* places is defined in an $n \times m$ incidence matrix *A*. An *m*-vector *Y* is called P-invariant if $A{\cdot}Y = 0$ and an *n*-vector *X* is called T-invariant if $A^T{\cdot}X = 0$. The support α_Y is a subset of places corresponding to the nonzero elements of P-invariant vector *Y*. One of the algebraic analysis approaches for obtaining the marking set of initial states M^{ini} is invariants of the net.

The DP can be illustrated based on the Petri net model as follows:

$$\mathrm{PNDP} = \left(N, P^{\mathrm{ini}}, P^{+}, P^{-}\right) \tag{4}$$

where *N*, P^{ini}, P^{+}, and P^{-} denote the Petri net model of the casual system, the initial states, the set of observations predicted by a solution, and the known set of absent findings. According to a theorem in [37], any marked PN has exactly one final marking; therefore, an initial marking M_0 is a solution to Petri net diagnosis problem if and only if the final marking *M* of *N* covers P^{+} and zero covers P^{-} according to the following definition. Given a Petri net $N = (P, T, F)$ and $Q \subseteq P$, a marking *M* covers *Q* if and only if $\forall p \in Q \rightarrow M(p) = 1$; while it zero-covers *Q* if and only if $\forall p \in Q \rightarrow M(p) = 0$.

C. Invariant-Based Diagnosis

The diagnosis process based on conventional reachability graph technique faces state-space explosion problem, especially in the consistency checking process even for small net models [32]. However, the reasoning scheme can be obtained effectively through the invariant process with symbolic and parallel computation. In this paper, P-invariant analysis is used for fault diagnosis. The causal behavior of a system is defined by the P-invariants of a net *N* which are generated offline such that the diagnostic result supports a set of manifestations.

The P-invariant vector exists for a Petri net $N = (P, T, F)$ based on the following lemma [37]. If place *p* is a sink place such that $\forall p \in P, |p^{\bullet}| = 0$, P-invariant *Y* ($Y(p) \neq 0$) of *N* is determined if and only if a firing sequence of transitions from an initial marking M_0 exists in which $M_0(s) \neq 0 \Rightarrow \forall s \in P, |{}^{\bullet}s| = 0$ (*s* is a marked initial state leads to manifest *p*).

Simplifying the original sketched net into an equivalent net is required before applying the algorithm. The places ended to AND transitions (T_N) in the original net are combined into a single place. It can be described as follows:

$\forall t \in T_N$ if ${}^\bullet t = \{p_1, \ldots, p_k\}(k > 1)$, then the set $\{p_1, \ldots, p_k\}$ in P is collapsed in the place $p_{1,k}$ such that ${}^\bullet p_{1,k} = \bigcup_{i=1}^{k} {}^\bullet p_i$ and $p^\bullet = \{t\}$.

According to [32], the invariant algorithm is applied to the simplified net. The minimal supports α_Y of P-invariants of the model are computed and those leading to marked places in Man^-, which are defined as $\forall p \in \text{Man}^-; \{\alpha_Y | \forall p \in \text{Man}^- \wedge p \in \alpha_Y\}$, are removed. Moreover, if μ and μ' are two sets of source places such that $\mu \subseteq \mu'$, and if the marking of μ leads to marking of the places of undesired observations (i.e., $p \in \text{Man}^-$), it can be concluded that the marking of μ' marks the same manifest p. Therefore, μ' should also be eliminated.

The final diagnose Δ for a certain DP is obtained by combining the initial places of the remaining supports that cover element of Man^+ $(p \in \text{Man}^+)$.

III. Distributed Diagnosis Approach

In a centralized fault-diagnosis method, the Petri net model for the entire power system is built and the observations throughout the power grid are sent to the central control center. A fault-diagnosis method that requires the global model of the system is not desirable for multiarea power systems as the system is operated by different power system operators who are reluctant to share the detailed model and real-time data of their associated subsystems. Distributed fault-diagnosis approaches are suitable solutions for such multiarea power systems. A distributed fault-diagnosis approach consists of a set of subsystems in which each subsystem has its own fault-diagnosis model and the local diagnosis result is achieved based on the local observations and limited information exchanged with the adjacent subsystems. The consistency of the local results is checked with the obtained results from neighboring subsystems and the inconsistent ones are discarded from the final solution.

The local diagnostic problem for area *i* can be defined as follows [7], [32], [41]:

$$\text{DP}_i = \left(\text{NM}_i,\ \text{Hyp}_i, \text{In}_i, \text{Out}_i, \text{Man}_i^+, \text{Man}_i^-\right) \tag{5}$$

where $\text{NM}_i, \text{Hyp}_i, \text{In}_i, \text{Out}_i$, and $\text{Man}_i^+, \text{Man}_i^-$ denote the local net model of the Area *i*, all local possible values of initial states in the Area *i* that cause the same findings, the input common elements from other areas to the area *i*, the output common elements to other areas from area *i*, and the local observations set, respectively. Since the causes of In_i belong to the Petri net of adjacent areas, it can be considered as the initial nodes for NM_i. On the contrary, the elements of Out_i can be viewed as the manifestations of NM_i because they can be represented as the causes of other effects which are modeled in the neighboring nets. Naturally, the Out_i set can be separated into two subsets, Out_i^+ that corresponds to the output values resulted from the local diagnosis Δ_i, and Out_i^- which corresponds to the values of undesired findings. A local diagnosis $\Delta_i \subseteq \text{Hyp}_i$ is determined to be consistent with the diagnoses of other neighbors if it covers all elements of Man_i^+, and Out_i^+ and do not cover any elements of Man_i^-, and Out_i^-. It can be described in a logical form as follows [42]:

$$\begin{aligned} &\forall\, w \in \text{Man}_i^+ \cup \text{Out}_i^+ : BM_i \cup \text{In}_i \cup \Delta_i \vdash w \\ &\forall\, v \in \text{Man}_i^- \cup \text{Out}_i^- : BM_i \cup \text{In}_i \cup \Delta_i \dashv v. \end{aligned} \tag{6}$$

Each subsystem is not completely independent, and it interacts with other subsystems via common mediums which are the places in the Petri net model. The common component belongs to two adjacent nets which captures interaction between them.

In the distributed fault-diagnosis approach, area *i* with interaction with the neighboring areas builds its own Petri net model which is represented as follows:

$$\text{PNDP}_i = \left(N_i, CP_i^{\text{In}}, CP_i^{\text{Out}}, P_i^+, P_i^-\right) \tag{7}$$

where $N_i = (P_i, T_i, F_i)$ is the Petri net model, CP_i^{In} is the set of common input places from other areas to the area *i*, and CP_i^{Out} denotes the sets of common output places form area *i* to other neighbors. P_i^+, P_i^- are the manifestations places of the subsystem *i*. The global Petri net model is the aggregation of all subsystem models with the following properties:

$$\begin{aligned} &N = (P, T, F) = \textstyle\bigcup_{i=1}^{n} N_i \\ &(i)\ P = \textstyle\bigcup_{i=1}^{n} P_i,\ \forall i \Rightarrow \exists j \text{ s.t. } P_i \cap P_j = P_{ij} \neq \varphi, \\ &\quad P_{ij} \subseteq CP_i^{\text{In}} \cup CP_i^{\text{Out}}. \\ &(ii)\ T = \textstyle\bigcup_{i=1}^{n} T_i,\ \forall i \neq j \Rightarrow T_i \cap T_j = \varphi. \\ &(iii)\ CP_i^{\text{In}} = \{p | (p^\bullet \in T_i) \wedge ({}^\bullet p \notin T_i)\}. \\ &(iv)\ CP_i^{\text{Out}} = \{p | (p^\bullet \in T_i) \wedge (p^\bullet \notin T_i)\}. \end{aligned} \tag{8}$$

The local diagnosis of each subsystem/area is obtained by reasoning the local observations and computing the minimal supports α_Y of P-invariants of the local net models. Then, to check the global consistency constraint between the diagnosis results of different subsystems/areas, the marking status of the required set of its common input places in CP_i^{In} (i.e., that necessitate to receive tokens from neighboring net models) is requested from the neighboring net models. The following message will be sent from Area *i* to its neighbors:

$$\text{Msg}_{i \to j} = \left\{p | p \in CP_i^{\text{In}} \cap P_{ij} \cap \alpha_Y \wedge \alpha_Y \in L_i\right\} \tag{9}$$

where L_i is the set of minimal supports of P-invariants of the net model of Area *i*. The message requests the marking status of place *p* which is member of intersection set of the common input places in Area *i* (CP_i^{In}), common places between area *i* and *j* and minimal supports (α_Y). Then, the receivers of the requests (adjacent areas) examine their remaining set of supports to check if the places contained in the received message is a member of at least one of their supports. The markings which are not confirmed by the neighboring diagnosis are eliminated from the final solution set.

IV. Proposed Fault Location Method

In the proposed fault location method, the location of the fault is identified in two stages. In the first stage, all possible faulty lines are identified using the Petri net algorithm that utilizes status data such as status of the output of protective relays and circuit breakers. Then, in the second stage, the identified short list of faulty lines in the first stage is further studied to identify the actual location of the fault. The actual location of the fault

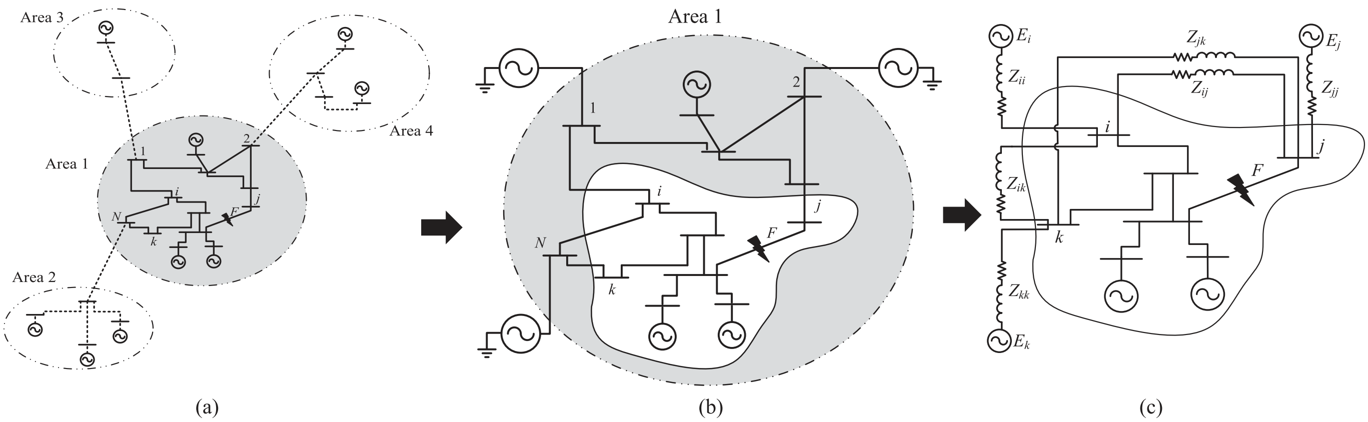

Fig. 2. Schematic diagram of the reduced network of multiarea power systems for fault study.

is determined based on the comparison between the voltage and current signals measured throughout the power grids during the fault period with simulated corresponding values generated by applying faults on the simulated network in a short-circuit analysis computer program. For reducing the number of simulations, binary search such as [43] and [44] can be also used that reduces the number of locations that faults should be applied. The proposed method can analyze various fault conditions. In other words, the fault type and fault resistance can be estimated utilizing the existence methods. For instance, Baldwin *et al.* [45] used directional ground fault indicators to identify high-resistance grounded fault location. Fault resistance (R_f) is estimated with extrapolation/interpolation procedure in [27]. Besides, the expert system method [46] and patterns of the voltage sag [47] have been developed to identify fault type. In this paper, knowing the fault type and fault resistance are considered as the presumptions.

To make the proposed two-stage fault location method applicable for multiarea power grids, it is implemented in a distributed architecture. The first stage is implemented using distributed Petri net which was explained in previous section.

To implement the second stage in a distributed architecture, the procedure depicted in Fig. 2 is followed. The fault-diagnosis system of Area#1 replaces the neighboring areas by voltage sources with the values equal to the measured voltages at boundary buses as shown in Fig. 2(b). Then, to reduce the computational burden of short-circuit analysis, the power grid of Area#1 is divided into the region under study and remaining network. The remaining network is replaced by its equivalent using the network reduction method presented in [48]. The equivalent network is calculated and represented as the multiple π-equivalents for the boundary nodes which the shunt branch consists of a voltage source behind a series impedance. The value of the voltage source is equal to the open-circuit voltage at that node and the impedance includes a constant resistance in series with a time-varying reactance which its value depends on the synchronous, transient and subtransient reactances at the boundary nodes [48].

The proposed two-stage fault location method is summarized as follows.

1) The first stage of the proposed fault location method determines a short list of possible faulty lines using distributed Petri nets that utilize status data.
2) In the second stage, analog measurements such as voltage and current signals are obtained from meters such as PMUs and conventional voltage and current meters that are installed throughout the power grid in the region under study.
3) The voltage and current signals at the meters' locations are calculated using a short-circuit analysis computer program. It is assumed that the fault has occurred on lines *i*–*j* between bus *i* and bus *j* and the fault distance from the bus *i* is xL_{ij}, where L_{ij} is the line length and $0 \leq x \leq 1$. This process is applied only to the lines that are in the short list that is determined by the first stage of the proposed fault location method.
4) The difference between magnitudes of the calculated and measured signals for $i = 1, 2, \ldots, N_r$ are calculated where N_r is the number of available meters

$$\delta_i\,(x) = \left|S_i^{\mathrm{cal}}\,(x)\right| - \left|S_i^{\mathrm{meas}}\right|. \tag{10}$$

5) The location of the fault is determined by minimizing all of the calculated matching degree $\delta_i(x)$ over all the possible fault locations by considering a step of Δx, where $x = k\Delta x$, $k = 1, 2, \ldots, 1/\Delta x$

$$\min_{x \in L_f} \sum_{i=1}^{N_r} \delta_i^2(x). \tag{11}$$

Thus, $x^* L_{ij}$ is the final fault location from the bus *i*. The matching degree index defined in (11) has the lowest value for the actual location of the fault.

V. Simulation Results

The performance of the proposed distributed fault diagnostic method is studied in this section. The proposed strategy is applied to the New-England 68 bus test system [49]. The one-line diagram of the system is shown in Fig. 3(a). The simulations are carried out on a 3.60-GHz computer with 16-GB RAM core i7 processor. According to the simulated cases, once a fault

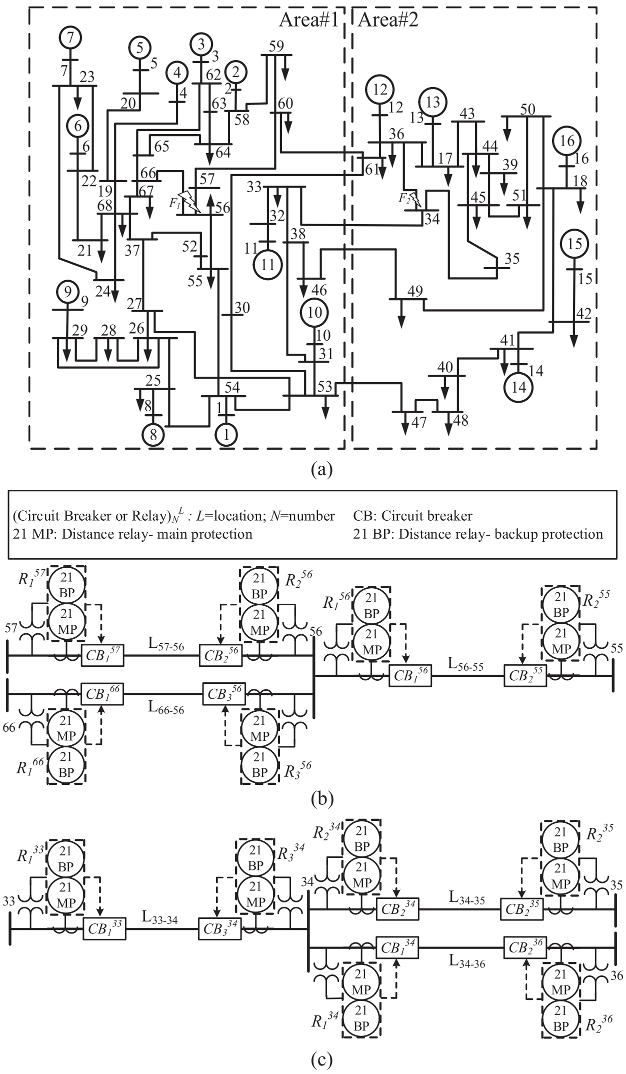

Fig. 3. Test power system and protection coordination philosophy. (a) IEEE 16-machine 68-bus system. (b) Main, local and RP for lines L_{57-66}, L_{66-56}, and L_{56-55}. (c) Main, local and RP for lines L_{33-34}, L_{34-35}, and L_{34-36}.

occurs, the proposed decentralized two-stage method calculates the fault location in matter of few seconds. Due to page limitation, only distance protection of transmission lines (ANSI 21) is considered in developing the Petri net of the modeled power system. The schematic diagram of installed protective devices in the vicinity of faults F_1 and F_2 is depicted in Fig. 3(b) and (c). The protection system consists of main primary protection relays, and local backup protection (BP) and remote backup protection (RP). The details of the coordination procedure can be found in [50]. In this study, it is assumed that at most one relay may fail to operate at a time. If the simultaneous failures of more than one relay are modeled, the Petri net of the system becomes larger which makes it difficult to explain the performance of the proposed method. Moreover, it is assumed that the status data of at most one operated relay may be lost.

The system is divided into two subsystems Area#1 and Area#2. The system is assumed to be divided according to the geographical areas of ownership by the system operators. The fault-diagnosis system of Area#1 is indicated by PN_1 and fault diagnostic system of Area#2 is indicated by PN_2.

Case 1: a simultaneous double fault (F_1) occurs on the transmission lines L_{57-56}, and L_{66-56} in Area#1 and relay R_3^{56} fails to operate while other protective devices operate correctly. The responses of relays R_1^{57}, R_2^{56}, R_1^{66}, and R_2^{55} and circuit breaker CB_1^{57}, CB_2^{56}, CB_1^{66}, and CB_2^{55} are observed in Area#1, while status of relays and circuit breakers of Area#2 are not affected by this fault. The Petri nets of the distributed fault diagnostic algorithm are depicted in Fig. 4 which corresponds to lines L_{57-56}, L_{66-56}, and L_{56-55} in Area# 1.

Petri net models for other components of the system can be built similarly. The PN_1 and PN_2 receive the local observed responses of the protection systems as follows:

$$\mathrm{Man}_1^+ = < P_{28}[b], P_{30}[b], P_{45}[b], P_{46}[b], P_{47}[b], P_{48}[b], P_{68}[b], P_{85}[b], P_{86}[b], P_{118}[b], P_{135}[b], P_{136}[b] >$$

$$\mathrm{Man}_2^+ = \langle \Phi \rangle .$$

Other finding places (i.e., observations) in the Petri net model do not receive any token and are members of the sets of undesired observations Man_1^-, Man_2^- in both areas. The depicted Petri nets are simplified by combining those input places of AND transitions that have the condition that was discussed in Section II-C. For instance, in Fig. 4(a), places P_{13} and P_{14} are replaced by place $P_{13\&14}$. PN_1 that are shown in Fig. 4(a)–(c) include 45 supports. For instance, the minimal supports of P-invariants for Petri net of line L_{57-56} are calculated as follows:

$$\sigma_1 = \{P_{10}, P_{11}, P_{13\&14}, P_{21}, P_{25}, P_{31\&32}, P_{43}\}$$
$$\sigma_2 = \{P_{10}, P_{11}, P_{13\&14}, P_{21}, P_{25}, P_{33\&34}, P_{44}\}$$
$$\sigma_3 = \{P_{10}, P_{11}, P_{13\&14}, P_{21}, P_{26}\}$$
$$\boldsymbol{\sigma_4} = \{P_{10}, P_{11}, P_{15\&16}, P_{22}, P_{27}, P_{35\&36}, P_{45}\}$$
$$\boldsymbol{\sigma_5} = \{P_{10}, P_{11}, P_{15\&16}, P_{22}, P_{27}, P_{37\&38}, P_{46}\}$$
$$\boldsymbol{\sigma_6} = \{P_{10}, P_{11}, P_{15\&16}, P_{22}, P_{28}\}$$
$$\boldsymbol{\sigma_7} = \{P_{10}, P_{12}, P_{17\&18}, P_{23}, P_{62}, P_{67}, P_{75\&76}, P_{85}\}$$
$$\boldsymbol{\sigma_8} = \{P_{10}, P_{12}, P_{17\&18}, P_{23}, P_{62}, P_{67}, P_{77\&78}, P_{86}\}$$
$$\boldsymbol{\sigma_9} = \{P_{10}, P_{12}, P_{17\&18}, P_{23}, P_{62}, P_{68}\}$$
$$\boldsymbol{\sigma_{10}} = \{P_{10}, P_{12}, P_{17\&18}, P_{23}, P_{112}, P_{117}, P_{125\&126}, P_{135}\}$$
$$\boldsymbol{\sigma_{11}} = \{P_{10}, P_{12}, P_{17\&18}, P_{23}, P_{112}, P_{117}, P_{127\&128}, P_{136}\}$$
$$\boldsymbol{\sigma_{12}} = \{P_{10}, P_{12}, P_{17\&18}, P_{23}, P_{112}, P_{118}\}$$
$$\boldsymbol{\sigma_{13}} = \{P_{10}, P_{12}, P_{19\&20}, P_{24}, P_{29}, P_{39\&40}, P_{47}\}$$
$$\boldsymbol{\sigma_{14}} = \{P_{10}, P_{12}, P_{19\&20}, P_{24}, P_{29}, P_{41\&42}, P_{48}\}$$
$$\boldsymbol{\sigma_{15}} = \{P_{10}, P_{12}, P_{19\&20}, P_{24}, P_{30}\}.$$

The remaining supports for two other Petri nets can be written similarly. Supports that contain places belonging to Man_1^- are discarded. For instance, the manifest P_{43} in the support σ_1 is a member of Man_1^-, and as a result it is eliminated from the diagnosis. Consequently, σ_1–σ_3, σ_{16}–σ_{18}, σ_{28}–σ_{33}, and σ_{43}–σ_{45}

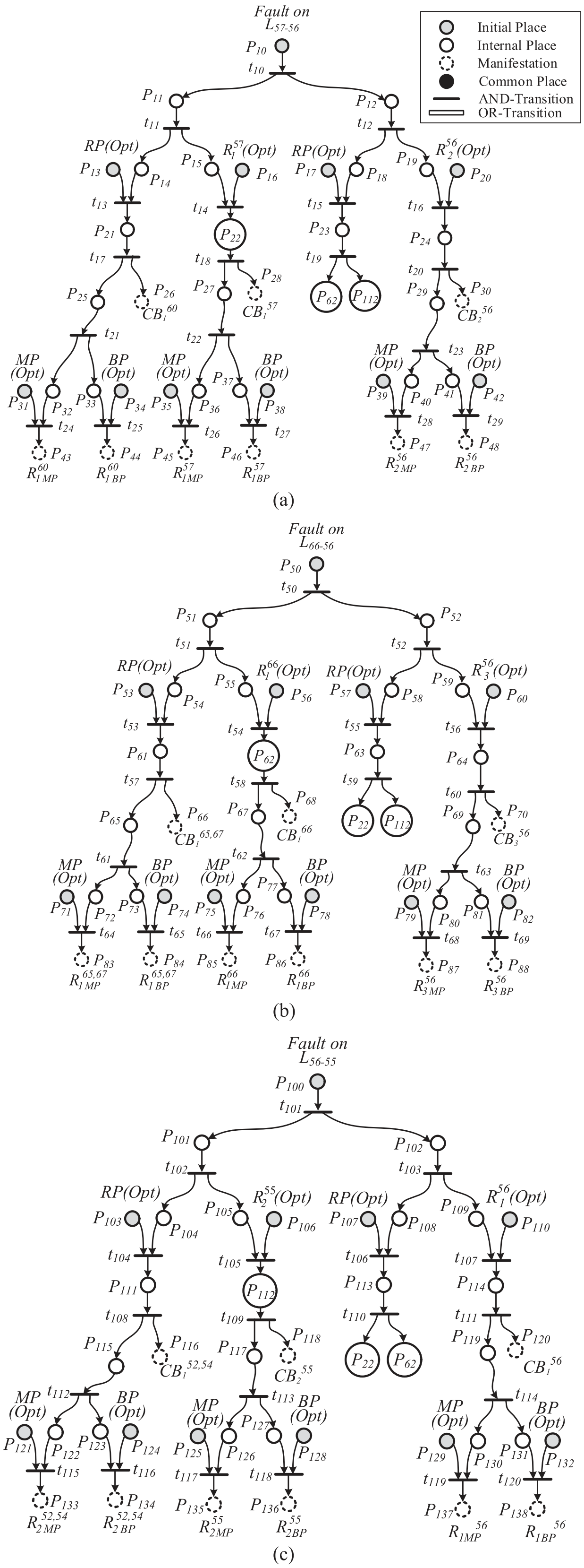

Fig. 4. Distributed fault-diagnosis model based on the Petri net for Case 1. (a) Petri net model (PN_1) for main, local backup, and RPs of line L_{57-56} in Area#1. (b) Petri net model (PN_1) for main, local backup, and RPs of line L_{66-56} in Area#1. (c) Petri net model (PN_1) for main, local backup, and RPs of line L_{56-55} in Area#1.

are discarded. Some of the supports that survive are bolded in the list. The remaining supports will be used to generate diagnoses for PN_1 which explain the local observations in Man_1^+. As a result, the observed symptoms in Area#1 are explained by the following local diagnoses:

$$\Delta_1^1 = \langle P_{10}, P_{16}, P_{20}, P_{35}, P_{38}, P_{39}, P_{42}, P_{50}, P_{56}, P_{75}, P_{78}, P_{125}, P_{128}\rangle$$

$$\Delta_2^1 = \langle P_{10}, P_{16}, P_{20}, P_{35}, P_{38}, P_{39}, P_{42}, P_{75}, P_{78}, P_{100}, P_{106}, P_{125}, P_{128}\rangle.$$

As in this fault scenario the common places are not members of the local diagnoses, therefore the marking status of the common places between areas is not required. Area#1 can perform the diagnosis process only based on its own Petri net model without any communication. The local diagnoses conclude a double fault that has been occurred in the system. The observations from main and local BP of L_{57-56} (i.e., R_2^{56} and R_1^{57}) and their related circuit breakers indicate that L_{57-56} is one of the faulted lines. The possible location of the other fault is either line L_{66-56} where relay R_3^{56} has failed to operate, or L_{56-55} where relay R_1^{56} has failed to operate. In the second stage of the proposed fault location method, the measured and calculated voltages and currents signals are utilized according to the procedure explained in Section IV to find the location of the faults. Accordingly, L_{66-56} is determined as the other faulted line. The matching degree, defined in (11), is 0.05 in this case.

Case 2: a fault (F_2) occurs on the transmission lines L_{34-36} in Area#2 and relay R_1^{34} fails to operate while other protective devices operate correctly. The status of relay R_1^{33} and circuit breaker CB_1^{33} are observed in Area#1, and Area#2 also receives signals from relays R_2^{35}, and R_2^{36} and circuit breakers CB_2^{35}, and CB_2^{36}. The Petri nets models are illustrated in Fig. 5 which corresponds to L_{33-34} in Area# 1, and L_{34-35}, L_{34-33}, and L_{34-36} in Area#2. The local observed manifestations in each area are as follows:

$$\text{Man}_1^+ = \langle P_{169}[b], P_{180}[b], P_{181}[b]\rangle$$

$$\text{Man}_2^+ = \langle P_{268}[u], P_{272}[b], P_{274}[b], P_{291}[b], P_{292}[b], P_{293}[u], P_{294}[u], P_{297}[b], P_{298}[b], P_{310}[u], P_{315}[u], P_{316}[u], P_{366}[u], P_{378}[u], P_{379}[u], \rangle.$$

The unobserved manifestations of the protective devices on these lines (relays R_1^{34}, R_2^{34} and R_3^{34} and circuit breakers CB_1^{34}, CB_2^{34} and CB_3^{34}) are marked as unknown status to consider the impact of lost data. Other findings do not receive any token and are members of the undesired observations sets Man_1^-, and Man_2^- in both areas. The minimal support sets can be calculated similar to the previous test case. PN_1 and PN_2 which are shown in Fig. 5(a)–(d) include 12 and 44 supports, respectively. The local diagnoses are computed after discarding the supports which contain undesired observations. According to the local results, the required marking status of the bordered places is obtained via a communication protocol between neighboring areas and the inconsistent diagnoses are discarded. The remaining supports in PN_1 that are determined by the local

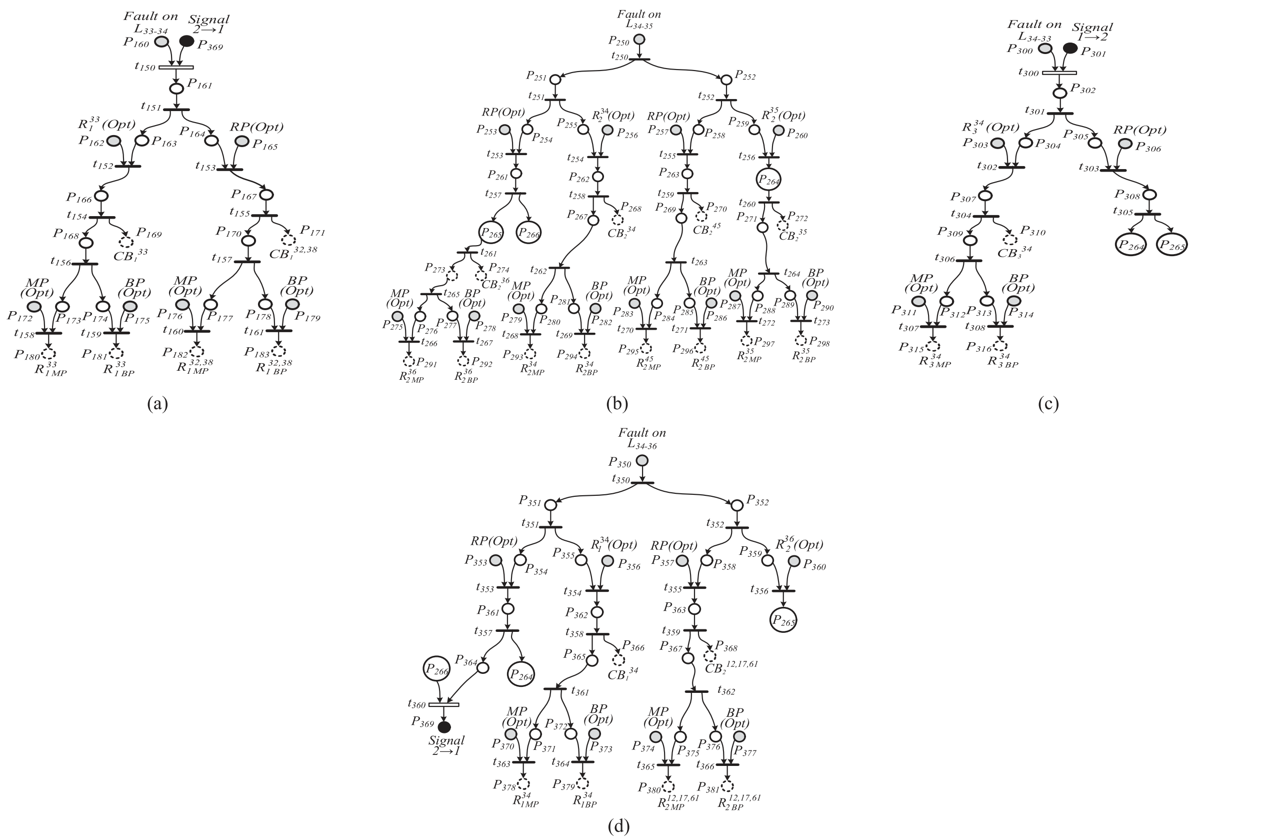

Fig. 5. Distributed fault-diagnosis model based on the Petri net for Case 2. (a) Petri net model (PN_1) for main, local backup, and RPs of line L_{33-34} in Area#1. (b) Petri net model (PN_2) for main, local backup, and RPs of line L_{34-35} in Area#2. (c) Petri net model (PN_2) for main, local backup, and RPs of line L_{34-33} in Area#2. (d) Petri net model (PN_2) for main, local backup, and RPs of line L_{34-36} in Area#2.

diagnoses are as follows:

$$\Delta_1^1 = \langle P_{160}, P_{162}, P_{172}, P_{175} \rangle$$
$$\Delta_1^2 = \langle P_{369}, P_{162}, P_{172}, P_{175} \rangle .$$

According to the computed diagnosis, the operations of relay R_1^{33} and circuit breaker CB_1^{33} in Area 1 are caused by local fault on tie-line L_{33-34} or an outside failure that is propagated from neighboring area. As it is assumed that PMUs are installed at both ends of the tie-lines, the location of faults on tie lines can be identified using PMUs data and are not considered in the proposed fault-diagnosis process. Therefore, the second result is the diagnosis for Area#1 which states that there is a fault in Area#2 causing some observations in PN_1 through common place P_{369}.

Applying the aforementioned procedure to Area#1, the manifestations in PN_2 can be described by the following diagnosis:

$$\Delta_2^1 = \langle P_{250}, P_{253}, P_{260}, P_{275}, P_{278}, P_{287}, P_{290} \rangle$$
$$\Delta_2^2 = \langle P_{250}, P_{350}, P_{260}, P_{275}, P_{278}, P_{279}, P_{282}, P_{287}, P_{290}, P_{256}, P_{360} \rangle$$
$$\Delta_2^3 = \langle P_{350}, P_{353}, P_{360}, P_{275}, P_{278}, P_{287}, P_{290} \rangle$$
$$\Delta_2^4 = \langle P_{350}, P_{253}, P_{360}, P_{275}, P_{278}, P_{287}, P_{290}, P_{356}, P_{370}, P_{373}, P_{250}, P_{260} \rangle .$$

The first diagnosed case refers to the scenario that a fault has occurred on L_{34-35} but relay R_2^{34} has failed to operate, and adjacent relays R_2^{35}, and R_2^{36} and circuit breakers CB_2^{35}, and CB_2^{36} in Area#2 and relay R_1^{33} and circuit breaker CB_1^{33} in Area#1 have detected and isolated the fault. The second diagnosed case refers to the scenario that a simultaneous double fault has occurred on L_{34-35} and L_{34-36}, but relay R_1^{34} has failed to issue a trip command to circuit breaker CB_1^{34} to clear the fault, and adjacent relays have detected and cleared the fault but the data from the correctly operated protective devices R_2^{34} and the corresponding circuit breaker CB_1^{34} are lost. The third diagnosed case refers to the scenario that a fault has occurred on L_{34-36} but relay R_1^{34} has failed to operate and other protective devices have cleared the fault correctly. The last case refers to a scenario that a double fault has occurred on L_{34-35} and L_{34-36} but relay R_2^{34} has failed to operate and the adjacent devices have detected and cleared the fault but the data from the correctly operated protective devices R_1^{34} and CB_1^{34} are lost.

After performing fault-diagnosis process based on the local observations, Area#1 sends a message to Area#2 and asks about the marking status of the common places that are used by Area#1 as the initial places for its local diagnose. As a result, Area#1 sends a message $\mathrm{Msg}_{1\rightarrow 2} = \{P_{369}\}$ to Area#2. Then, Area#2 checks whether the received bordered place (P_{369}) from Area#1 belongs to the remaining set of supports of Area#2. According to the local computations in Area#2, P_{369} is the observation of

TABLE I
RANKING OF THE FIRST STAGE DIAGNOSES FOR CASE 2

Diagnoses	Faulted Line	Failed Relay	Lost Data	Matching Degree
Δ_2^3	$L_{34\text{-}36}$	R_1^{34}	–	0.06
Δ_2^4	$L_{34\text{-}35}$ & $L_{34\text{-}36}$	R_2^{34}	R_1^{34} & CB_1^{34}	20.45
Δ_2^1	$L_{34\text{-}35}$	R_2^{34}	–	60.23
Δ_2^2	$L_{34\text{-}35}$ & $L_{34\text{-}36}$	R_1^{34}	R_2^{34} & CB_2^{34}	220.74

supports of Area#2. Therefore, Area#2 concludes that there is a consistency between its diagnosis and the received message from Area#1 and sends a positive response to Area#1.

By using the aforementioned procedure, the first stage of the proposed fault location method concludes that four different scenarios ($\Delta_2^1 - \Delta_2^4$) are viable cases for the fault. Then, in the second stage of the proposed fault location method, the actual location of the fault is determined. Table I shows the values of matching degrees for these four scenarios. The matching degree has the lowest value (0.06) for the actual fault case which belongs to the fault scenario that a single fault has occurred on L_{34-36} in Area#2 but relay R_1^{34} has failed to operate. The second contingency with matching degree 20.45 belongs to the double fault on L_{34-35} and L_{34-36} and relay R_2^{34} has failed to operate while the data from the correctly operated protective devices R_1^{34} and CB_1^{34} are lost. The next scenario with calculated matching degree 60.23 is a single fault on

L_{34-35} and relay R_2^{34} has failed to operate. The last diagnosis in this list with the matching degree 220.74 is the simultaneous double fault on L_{34-35} and L_{34-36}, and relay R_1^{34} has misoperated to issue a trip command to circuit breaker CB_1^{34}, and the data from the correctly operated protective devices R_2^{34} and the corresponding circuit breaker CB_1^{34} are lost.

VI. DISCUSSIONS

In comparison to the pervious methods, the main contributions of the proposed method in this paper can be summarized as follows.

1) The proposed two-stage fault location identification approach calculates the actual fault location in multiarea power grids in a distributed method. Therefore, each system operator finds the solution for its own subsystem locally and only limited information is exchanged with neighboring subsystems to eliminate inconsistent results from the local diagnosis. The proposed method is in contrast to the previous fault-diagnosis algorithms which build the global model of the entire system and diagnose the faults in a centralized approach which is not applicable to multiarea power systems operated by different system operators.
2) The proposed method provides a systematic approach for using all available data including status data and analog data. Status data such a status of circuit breakers and output of protective relays are used as the observations for the Petri net model. The short list of the faulted sections generated by the Petri net method narrows down the search area for the second stage of the proposed method. Analog data such as voltage and current signals measured by PMUs or conventional meters are utilized in the second stage to determine the actual fault location and eliminate possible falsely estimated sections by the first stage due to loss of data or failure of protective relays. Therefore, the proposed method takes full advantage of both types of data to reduce the computation burden and speed up the fault location identification procedure and eliminate false section identifications in the presence of failures of protective relays.
3) The MBD method based on P-invariant Petri net is proposed to find the potential faulted sections. In comparison to the other Petri net methods [51]–[53], P-invariant Petri net reduces the computation burden and speeds up the calculation procedure by simplifying the original sketched net into an equivalent net and discarding the supports which leads to the undesired manifestations.
4) The diagnosis process based on conventional reachability graph technique faces state-space explosion problem, especially in the consistency-checking process that even for small net model state-space explosion problem may occur [32]. However, P-invariant reasoning scheme can define the casual behavior of the system for large-scale net models.
5) Failures of the protective devices (relays and circuit breakers) and data lost can be considered in the proposed fault-diagnosis algorithms.
6) The proposed fault location method provides the best results for available data. If the number of measurements is very small, there are cases that two fault locations may provide the same characteristics at the measurement locations and cannot be distinguished. To address this issue, the number of meters should be increased or strategically installed at certain locations to provide best results. If still the results cannot be improved, similar to other fault location methods, the proposed method provides the short list of estimated fault locations to the operator for further analysis by dispatching the crew.
7) The proposed algorithm is flexible and can utilize the model of protection schemes of other components (such as bus bar protection, transformer protection). As the model has a modular architecture, the causal model of the new protection scheme can be added to the already existing model. Therefore, the proposed method can not only localize fault in the transmission lines but also in other components of the systems.
8) To deal with possible noise or uncertainties, fuzzy logic algorithms or Bayesian theorem can be combined with the Petri to improve the results.

VII. CONCLUSION

In this paper, a two-stage distributed fault-diagnosis method for multiarea power systems was proposed. The proposed method is based on the casual properties of the Petri net model and similarity check between calculated and measured signals from power grids. The proposed method utilizes both status and analog data for the fault location purpose. In the proposed method for multiarea power systems, the fault-diagnosis system of each area analyzes the corresponding local Petri net model based on P-invariant algorithm and checks the consistency of the local explanations with external information coming from the adjacent areas. Only marking status of the common bordered places needs to be exchanged between neighboring subsystems/areas. The obtained diagnosis results that are inconsistent with the exchanged information with the neighboring areas are eliminated from the results. The diagnosis results are further improved by comparing the measured analog data such as voltage and current signals, with their corresponding simulated values. The performance of the proposed two-stage distributed fault-diagnosis method was studied by simulating different fault scenarios in the 68 bus New England system. The simulation results demonstrated the effectiveness of the proposed method in identifying the location of faults.

References

[1] M. Kezunovic and Y. Guan, "Intelligent alarm processing: From data intensive to information rich," in *Proc. 42nd Hawaii Int. Conf. Syst. Sci.*, Big Island, HI, USA, 2009, pp. 1–8.

[2] D. Durocher, "Language: An expert system for alarm processing," in *Proc. 11th Biennial IEEE Workshop Power Syst. Control Centers*, Montreal, PQ, Canada, Sep. 1990, pp. 19–21.

[3] S. Lotfifard, "Sparse sensing platform for line-outage identification in multiarea power systems," *IEEE Trans. Ind. Informat.*, vol. 13, no. 3, pp. 947–955, Jun. 2017.

[4] P. Kundu and A. K. Pradhan, "Real-time analysis of power system protection schemes using synchronized data," *IEEE Trans. Ind. Informat.*, vol. 14, no. 9, pp. 3831–3839, Sep. 2018.

[5] X. Dai and Z. Gao, "From model, signal to knowledge: A data-driven perspective of fault detection and diagnosis," *IEEE Trans. Ind. Informat.*, vol. 9, no. 4, pp. 2226–2238, Nov. 2013.

[6] R. Reiter, "A theory of diagnosis from first principles," *Artif. Intell.*, vol. 32, no. 1, pp. 57–95, 1987.

[7] Y. M. Berghout, "Probabilistic model-based diagnosis of distributed systems," Ph.D. dissertation, Dept. Comput. Sci., Mohamed Khider Univ., Biskra, Algeria, 2017.

[8] Y. C. Huang, "Fault section estimation in power systems using a novel decision support system," *IEEE Trans. Power Syst.*, vol. 17, no. 2, pp. 439–444, May 2002.

[9] H. J. Lee, B. S. Ahn, and Y. M. Park, "A fault diagnosis expert system for distribution substations," *IEEE Trans. Power Del.*, vol. 15, no. 1, pp. 92–97, Jan. 2000.

[10] Y. Zhang, C. Y. Chung, F. Wen, and J. Zhong, "An analytic model for fault diagnosis in power systems utilizing redundancy and temporal information of alarm messages," *IEEE Trans. Power Syst.*, vol. 31, no. 6, pp. 4877–4886, Nov. 2016.

[11] H. T. Yang, W. Y. Chang, and C. L. Huang, "A new neural networks approach to on-line fault section estimation using information of protective relays and circuit breakers," *IEEE Trans. Power Del.*, vol. 9, no. 1, pp. 220–230, Jan. 1994.

[12] C. Rodriguez, S. Rementeria, J. I. Martin, A. Lafuente, J. Muguerza, and J. Perez, "A modular neural network approach to fault diagnosis," *IEEE Trans. Neural Netw.*, vol. 7, no. 2, pp. 326–340, Mar. 1996.

[13] Y. Zhu, L. Huo, and J. Lu, "Bayesian networks-based approach for power systems fault diagnosis," *IEEE Trans. Power Del.*, vol. 21, no. 2, pp. 634–639, Apr. 2006.

[14] Q. Wen, X. Gu, and W. Li, "Information fusion method of multi-data resources and its application to fault diagnosis in power system," in *Proc. IET Renewable Power Gener. Conf.*, Beijing, China, Sep. 2013, pp. 1–4.

[15] C. L. Hor, P. A. Crossley, and S. J. Watson, "Building knowledge for substation-based decision support using rough sets," *IEEE Trans. Power Del.*, vol. 22, no. 3, pp. 1372–1379, Jul. 2007.

[16] W. H. Chen, C. W. Liu, and M. S. Tsai, "On-line fault diagnosis of distribution substations using hybrid cause-effect network and fuzzy rule-based method," *IEEE Trans. Power Del.*, vol. 15, no. 2, pp. 710–717, Apr. 2000.

[17] H. Miao, M. Sforna, and C. C. Liu, "A new logic-based alarm analyzer for on-line operational environment," *IEEE Trans. Power Syst.*, vol. 11, no. 3, pp. 1600–1606, Aug. 1996.

[18] Y. M. Park, G. W. Kim, and J. M. Sohn, "A logic-based expert system (LBES) for fault diagnosis of power system," *IEEE Trans. Power Syst.*, vol. 12, no. 1, pp. 363–369, Feb. 1997.

[19] A. T. Ghainani, A. A. M. Zin, and N. A. M. Ismail, "Fuzzy timing petri net for fault diagnosis in power system," *J. Math. Probl. Eng.*, vol. 2012, pp. 1–12, 2012.

[20] X. Wang and T. Dillon, "A second generation expert system for fault diagnosis," *Int. J. Elect. Power Energy Syst.*, vol. 14, nos. 2/3, pp. 212–216, 1992.

[21] K. L. Lo, H. S. Ng, D. M. Grant, and J. Trecat, "Extended Petri net models for fault diagnosis for substation automation," *Proc. Inst. Elect. Eng., Gener. Transmiss. Distrib.*, vol. 146, no. 3, pp. 229–234, May 1999.

[22] C. N. Hadjicostis and G. C. Verghese, "Power system monitoring using Petri net embeddings," *Proc. Inst. Elect. Eng. Gener. Transmiss. Distrib.*, vol. 147, no. 5, pp. 299–303, Sep. 2000.

[23] X. Zhang, S. Yue, and X. Zha, "Method of power grid fault diagnosis using intuitionistic fuzzy Petri nets," *IET Gener. Transmiss. Distrib.*, vol. 12, no. 2, pp. 295–302, Jan. 30, 2018.

[24] X. Luo and M. Kezunovic, "Implementing fuzzy reasoning Petri-nets for fault section estimation," *IEEE Trans. Power Del.*, vol. 23, no. 2, pp. 676–685, Apr. 2008.

[25] J. Sun, S. Y. Qin, and Y. H. Song, "Fault diagnosis of electric power systems based on fuzzy Petri nets," *IEEE Tran. Power Syst.*, vol. 19, no. 4, pp. 2053–2059, Nov. 2004.

[26] M. Kezunovic, "Smart fault location for smart grids," *IEEE Trans. Smart Grid*, vol. 2, no. 1, pp. 11–22, Mar. 2011.

[27] S. Lotfifard, M. Kezunovic, and M. J. Mousavi, "Voltage sag data utilization for distribution fault location," *IEEE Trans. Power Del.*, vol. 26, no. 2, pp. 1239–1246, Apr. 2011.

[28] Y. Liao, "Fault location for single-circuit line based on bus-impedance matrix utilizing voltage measurements," *IEEE Trans. Power Del.*, vol. 23, no. 2, pp. 609–617, Apr. 2008.

[29] H. Jiang, J. J. Zhang, W. Gao, and Z. Wu, "Fault detection, identification, and location in smart grid based on data-driven computational methods," *IEEE Trans. Smart Grid*, vol. 5, no. 6, pp. 2947–2956, Nov. 2014.

[30] H. Bennoui, "Interacting behavioral Petri nets analysis for distributed causal model-based diagnosis," *Auton. Agents Multi-agent Syst.*, vol. 28, no. 2, pp. 155–181, 2014.

[31] Z. Galijasevic and A. Abur, "Fault location using voltage measurements," *IEEE Trans. Power Del.*, vol. 17, no. 2, pp. 441–445, Apr. 2002.

[32] S. S. Gururajapathy, H. Mokhlis, and H. A. Illias, "Fault location and detection techniques in power distribution systems with distributed generation: A review," *Renewable Sustain. Energy Rev.*, vol. 74, pp. 949–958, 2017.

[33] Y. Liao, "Fault location utilizing unsynchronized voltage measurements during fault," *Elect. Power Compon. Syst.*, vol. 34, no. 12, pp. 1283–1293, Dec. 2006.

[34] L. Console and P. Torasso, "Hypothetical reasoning in causal models," *Int. J. Intell. Syst.*, vol. 5, no. 1, pp. 83–124, 1990.

[35] Z. Liu and K. Hu, "A model-based diagnosis system for a traction power supply system," *IEEE Trans. Ind. Informat.*, vol. 13, no. 6, pp. 2834–2843, Dec. 2017.

[36] C. A. Petri, Kommunikation Mit Automaten, 1962.

[37] L. Portinale, "Behavioral Petri nets: A model for diagnostic knowledge representation and reasoning," *IEEE Trans. Syst. Man, Cybern. B, Cybern.*, vol. 27, no. 2, pp. 184–195, Apr. 1997.

[38] K. L. Lo, H. S. Ng, and J. Trecat, "Power systems fault diagnosis using Petri nets," *IEE Proc. Gener. Transmiss. Distrib.*, vol. 144, no. 3, pp. 231–236, May 1997.

[39] T. Murata, "Petri nets: Properties, analysis and applications," *Proc. IEEE*, vol. 77, no. 4, pp. 541–580, Apr. 1989.

[40] L. Portinale, "Exploiting T-invariant analysis in diagnostic reasoning on a Petri net model," in *Proc. 14th Int. Conf. Appl. Theory Petri Nets*, Chicago, IL, USA, 1993, pp. 339–356.

[41] M. S. Rahman, M. A. Mahmud, A. M. T. Oo, and H. R. Pota, "Multiagent approach for enhancing security of protection schemes in cyberphysical energy systems," *IEEE Trans. Ind. Informat.*, vol. 13, no. 2, pp. 436–447, Apr. 2017.

[42] G. Jiroveanu and R. K. Boel, "Petri net model-based distributed diagnosis for large interacting systems," in *Proc. 16th Int. Workshop Principles Diagnosis*, 2005, pp. 25–30.

[43] D. K. Ranaweera, "Comparison of neural network models for fault diagnosis of power systems," *Elect. Power Syst. Res.*, vol. 29, pp. 99–104, 1994.

[44] A. Esmaeilian and M. Kezunovic, "Fault location using sparse synchrophasor measurement of electromechanical-wave oscillations," *IEEE Trans. Power Del.*, vol. 31, no. 4, pp. 1787–1796, Aug. 2016.

[45] T. Baldwin, F. Renovich Jr., and L. F. Saunders, "Directional ground fault indicator for high-resistance grounded systems," *IEEE Trans. Ind. Appl.*, vol. 39, no. 2, pp. 325–332, Mar./Apr. 2003.

[46] M. Kezunovic, P. Spasojevic, C. Fromen, and D. Sevcik, "An expert system for transmission substation event analysis," *IEEE Trans. Power Del.*, vol. 8, no. 4, pp. 1942–1949, Oct. 1993.

[47] H. Mokhlis, M. Hasmaini, H. Li, and A. A. Bakar, "Voltage sags matching to locate faults for underground distribution networks," *Adv. Elect. Comput. Eng.*, vol. 11, pp. 43–48, 2011.

[48] N. Tleis, *Power Systems Modelling and Fault Analysis*, 1st ed. Amsterdam, The Netherlands: Elsevier, 2008, pp. 485–496.

[49] B. Pal and B. Chaudhuri, *Robust Control in Power Systems*. New York, NY, USA: Springer, 2005.

[50] S. Horowitz and A. G. Phadke, *Power System Relaying*, 4th ed. New York, NY, USA: Wiley, 2014.

[51] X. Luo and M. Kezunovic, "Implementing fuzzy reasoning Petri-nets for fault section estimation," *IEEE Trans. Power Del.*, vol. 23, no. 2, pp. 676–685, Apr. 2008.

[52] J. Sun, S. Y. Qin, and Y. H. Song, "Fault diagnosis of electric power systems based on fuzzy Petri nets," *IEEE Tran. Power Syst.*, vol. 19, no. 4, pp. 2053–2059, Nov. 2004.

[53] X. L. Zhao, J. Z. Zhou, B. Fu, and H. Liu, "Research of probability Petri nets model for fault diagnosis based on Bayesian theorem," in *Proc. 7th World Congr. Intell. Control Automat.*, Chongqing, China, Jun. 2008, pp. 6253–6258.

Iman Kiaei (S'09–M'18) received his Ph.D. degree in electrical engineering from School of Electrical Engineering and Computer Science, Washington State University, Pullman, WA, in 2018. He has served as a reviewer for IEEE TRANSACTIONS journals and IEEE conferences.

Currently, he is the Associate System Planning Engineer at the New York Power Authority, White Plains, NY, USA. His research interests include power systems operation and planning, protection and control, fault location and diagnosis, and stability studies of power system.

Saeed Lotfifard (S'08–M'11–SM'17) received the Ph.D. degree in electrical engineering from Texas A&M University, College Station, TX, USA, in 2011.

He is currently an Assistant Professor with Washington State University, Pullman, WA, USA. His research interests include power system protection and control.

Dr. Lotfifard is an Editor for the IEEE TRANSACTIONS ON SMART GRID.